https://doi.org/10.31436/iiumej.v26i2.3577

VOLTAGE-INDUCED VOID FORMATION IN HIGH-TEMPERATURE OXIDE SCALES OF BOILER TUBES

MUHAMMAD RAFIQ HAIKAL ROSDIN[1], SYED NOH SYED ABU BAKAR[2], ABD MALEK ABDUL HAMID[1], AHMAD ABDUL MUN'IM ISMAIL[1], MOHD HANAFI ANI[1*]

[1]Department of Manufacturing and Materials Engineering, Kulliyyah of Engineering, International Islamic University Malaysia, 53100 Gombak, Selangor, Malaysia
[2]Department of Mechanical Engineering, Kulliyyah of Engineering, International Islamic University Malaysia, 53100 Gombak, Selangor, Malaysia

**Corresponding author: mhanafi@iium.edu.my*

(Received: 15 January 2025; Accepted: 8 April 2025; Published online: 15 May 2025)

ABSTRACT: Corrosion monitoring remains a significant challenge at high temperatures. Understanding the varying factors in high-temperature cathodic protection is crucial for developing mitigation strategies and predictive maintenance. This study assesses how cathodic protection influences oxidation in T91 alloys at elevated temperatures by evaluating the effects of exposure duration and voltage-induced void development in the oxide layer. It is hypothesized that polarizing the sample affects the diffusivity of cations and anions in the oxide scale, which is the rate-determining step of the oxidation process. This study measured the number of voids directly on T91 alloys exposed at 823K under various induced voltages. T91 alloy was externally induced with voltages of 0V, 50V, and 300V for 43.2 ks, 259.2 ks, and 432 ks at 923 K in air (P_{O_2}= 0.21 atm = 2.1×10^4 Pa). The presence of oxide layers was analysed using X-Ray Diffraction (XRD), and the void formed was inspected using Scanning Electron Microscopy (SEM). XRD results reveal that Fe_2O_3, Fe_3O_4, $FeCr_2O_3$, and Cr_2O_3 peaks were formed on all samples. The parabolic rate constant, K_p, was calculated as 3.83 × 10^{-14} m^2/s, 2.17 × 10^{-14} m^2/s, and 9.25 × 10^{-14} m^2/s, respectively, verifying that the reaction occurred by solid-state diffusion. Changes in K_p at different induced voltages are clear evidence that the diffusivity was altered by external electrical potential. It was observed that the overall void formation decreased by 17%. Inducing voltage onto T91 alloy affects the ionic diffusivity. It changes the void formation, suggesting it may promote the diffusivity of more inert species, such as Cr, to form a protective layer at the early oxidation stage.

ABSTRAK: Pemantauan hakisan kekal sebagai cabaran utama pada suhu tinggi. Memahami pelbagai faktor perlindungan katodik pada suhu tinggi adalah penting untuk membangunkan strategi pengurangan dan ramalan penyelenggaraan. Kajian ini menilai perlindungan katodik mempengaruhi pengoksidaan dalam aloi T91 pada suhu tinggi dengan melihat kesan tempoh pendedahan dan pembangunan rongga yang disebabkan oleh potensi elektrik luaran pada lapisan oksida. Pemolaran sampel mempengaruhi keberaliran kation dan anion dalam oksida, yang menentukan kadar dalam proses pengoksidaan. Melalui kajian ini, jumlah ruang kosong diukur secara langsung pada aloi T91 yang didedahkan pada suhu 823K di bawah pelbagai voltan teraruh. Aloi T91 dikenakan voltan luaran sebanyak 0V, 50V, dan 300V bagi tempoh 43.2 ks, 259.2 ks, dan 432 ks pada suhu 923K dalam udara (P_{O_2} = 0.21 atm = 2.1 × 10^4 Pa). Kehadiran lapisan oksida dianalisa menggunakan Pembelauan Sinar-X (XRD), dan ruang kosong yang terbentuk diperiksa menggunakan Mikroskop Elektron Imbasan (SEM). Dapatan XRD menunjukkan bahawa puncak Fe_2O_3, Fe_3O_4, $FeCr_2O_3$, dan Cr_2O_3 terbentuk pada semua sampel. Pemalar kadar parabola, K_p, dikira masing-masing sebanyak 3.83 × 10^{-14} m²/s, 2.17 × 10^{-14} m²/s, dan 9.25 × 10^{-14} m²/s, mengesahkan bahawa tindak balas yang berlaku adalah

penyebaran keadaan pepejal. Perubahan dalam K_p pada voltan teraruh berbeza membuktikan bahawa keberaliran telah diubah oleh potensi elektrik luaran. Hasil kajian mendapati bahawa pembentukan ruang kosong secara keseluruhan berkurangan sebanyak 17%. Proses penguraian voltan pada aloi T91 mempengaruhi keberaliran ionik dan mengubah pembentukan ruang kosong, mencadangkan bahawa ia mungkin digunakan bagi mempromosi keberaliran spesies yang lebih lengai seperti Cr bagi membentuk lapisan pelindung pada peringkat awal pengoksidaan.

KEYWORDS: *high temperature oxidation, T91 Alloy, void formation, induced voltage*

1. INTRODUCTION

The most economical method of producing hydrogen is through steam methane reforming (SMR), which accounts for 95% of global hydrogen production with an efficiency of 85% [1]. SMR involves reacting pure methane with superheated steam in the presence of a nickel catalyst to produce syngas. The steam is generated at 923K using a heat recovery steam generator (HRSG). Seamless ferritic alloy tubes, specifically T91 alloy (ASME SA-213 grade T91), are the common boiler tubes used in the HRSG system. These tubes are exposed to high temperatures, leading to oxidation in the presence of oxygen, which causes fouling and spalling of oxide scales. Although these tubes are designed to last 100,000 service hours, studies by Li et al. [2] show degradation starting as early as 4,000 hours, raising safety and operational concerns.

Research done by Maruyama et al. [3] had linked void formation in oxide scales during high-temperature oxidation to divergence of ionic flux. In a related study, Maruyama et al. [4] also examined void formation in growing oxide scales with Schottky defects and p-type conduction, finding that voids preferentially form near the metal/scale interface, their volume increases parabolically, and their volume fraction remains time-independent. Using the Nernst-Planck equation, Schlögl and Helffreich [5] theorized changes in ionic diffusivity under electrical potential. Further, Jin et al. [6] had analysed the influence of applied electric fields on carrier distribution during high-temperature corrosion, concluding that positive electric fields promote cation vacancy migration toward the metal interface, thereby altering the growth rate of corrosion film. However, the impact of electric fields on high-temperature corrosion remains underexplored. This study investigates how applied voltages (0V, 50V, and 300V) at 923K in normal air affect void formation in T91 alloy, aiming to understand the relationship between induced electrical potential and high-temperature corrosion.

2. EXPERIMENTAL METHODS

2.1. Sample Preparations

T91 alloy was cut into smaller pieces before being further cut into an average dimension of 10.9 mm × 6.4 mm × 4.2 mm using a precision saw machine. Then, it was ground using a grinding machine with various abrasive paper grades (P600 – P2000). A polishing machine was used to polish the ground sample using up to 0.3 micron-sized diamond particles.

2.2. Voltage-Induced Experiment

Figure 1 shows the schematic diagram for the experimental setup. A platinum wire of 1 metre length was used as the working and counter electrode. Platinum was chosen due to its high resistivity towards corrosion, high electrical conductivity, and low chemical reactions at high temperatures. Then, the T91 alloy sample was spot welded onto the working electrode.

https://doi.org/10.31436/iiumej.v26i2.3577

This was done to ensure the electrodes remained firmly in place during the experiment. An R-Type thermocouple was placed in the isothermal zone, 5mm from the sample, to measure precise temperature in the zone. Then, heat was supplied by the furnace.

The platinum electrodes were then connected to the Cockroft-Walton circuit, also known as a voltage multiplier. The amount of voltage supplied to the sample was 0V, 50V, and 300V. The experiment was conducted at 1 atm (2.1×10^4 Pa of oxygen) with standard dry air composition. For 20 minutes, the temperature was progressively raised to 923K to ensure stability inside the heated space. It was then left alone for another 15 minutes to check that the provided voltage is stable. Table 1 summarizes the parameters used for the experiment.

Table 1. Parameters used for the experiment.

Time (ks)	Voltage Supplied (V)
43.2	0
	50
	300
259.2	0
	50
	300
432	0
	50
	300

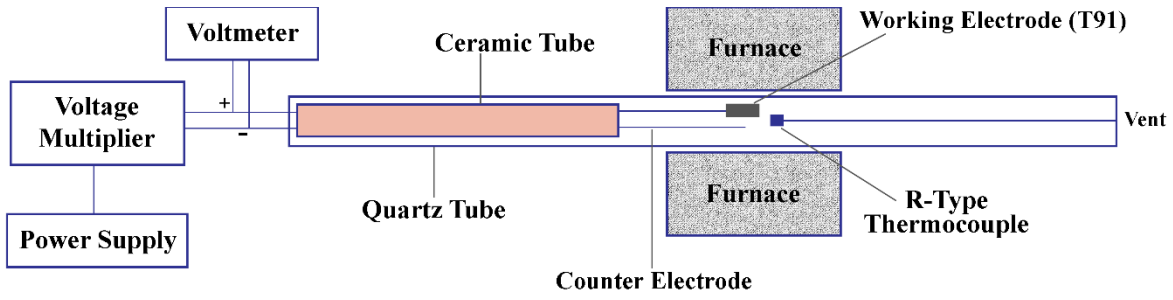

Figure 1. Schematic diagram for the Voltage Induced Experiment.

The selection of applied voltages was based on their expected impact on oxidation behaviour. 0V was a control condition, representing natural oxidation without external electric influence. 50V was chosen as a moderate voltage level, simulating conditions where minor electric fields could affect ionic mobility and void formation. 300V was selected to represent high-field conditions and evaluate whether the oxidation kinetics would still follow the parabolic rate constant (K_p) behaviour, which is typically observed in high-temperature oxidation. Deviations from the parabolic trend would indicate the presence of alternative mechanisms influencing oxidation under high-voltage conditions.

The exposure times of 43.2 ks (12 hours), 259.2 ks (72 hours), and 432 ks (120 hours) were selected to capture different oxidation stages. 43.2 ks represents the early-stage oxidation behaviour and initial void formation. 259.2 ks provides insight into progressive oxide scale growth and void evaluation. 432 ks enables observation of long-term oxidation effects, including steady-state oxide growth and potential saturation of void formation. However, common high-temperature corrosion studies often involve exposure periods longer than suggested durations, extending beyond 432 ks.

2.3. Phase Characterization

Oxide phases were analysed using XRD with divergence slit of 2.5 degree. The diffraction angle was set from 20° to 80°. Cross-sectional images generated by SEM were used to determine the oxide thickness, void formation, and parabolic rate constant.

The methodology of calculating volume fraction of voids was adopted from Kaderi et al. [7], wherein uniformly sized grids were superimposed onto the SEM images of oxide scale cross-sections. The area fraction of voids was calculated by assessing the proportion of void areas relative to the total oxide scale area within these grids, which was a standard approach in such analyses. To ensure measurement accuracy, multiple images were analysed for each sample to account for variability and enhance statistical stability. This method provides a reasonable estimation of void volume fractions.

3. RESULTS AND DISCUSSIONS

3.1. XRD Analysis

Figure 2 shows XRD patterns of all sample surfaces at respective conditions. The XRD analysis of the raw sample shows intensity peaks at diffraction angles of 44.8° and 65°, which confirms the presence of α-Fe in the BCC structure [8]. Furthermore, there are also noticeable peaks of Fe_2O_3 (hematite), Fe_3O_4 (magnetite), $FeCr_2O_3$ (spinel), and Cr_2O_3 (chromium), confirming that major phases have been identified.

Meanwhile, samples subjected to 300V for 43.2 ks and all samples exposed for 259.2 ks and 432 ks began to show a less intense peak of magnetite due to their variations in crystal structure and atom arrangement. Nasrazadani and Raman [9] stated that magnetite is a mixed valence iron oxide containing both Fe^{2+} and Fe^{3+} ions in an inverse spinel structure, while hematite has a corundum structure with only Fe^{3+} ions. Fe^{2+} ions in magnetite cause more disorder in the crystal structure, causing magnetite to have weaker diffraction peaks than hematite. The dense formation of hematite can also affect the XRD in detecting the magnetite phase [10].

The peaks of chromia started to increase from the sample exposed at 50V for 43.2 ks until 300V for 432 ks. However, the peak was less intense than magnetite and hematite. The presence of multiple phases can lead to a reduction in diffraction peaks. Other than that, the chromium content of T91 alloy was quite low at 9%, which can also lead to reduced intensity.

The XRD results demonstrate that increasing applied voltage influences the phase composition of the oxide scale, particularly by altering the formation and stability of magnetite and hematite. The observed reduction in magnetite intensity at higher voltage suggests potential changes in oxidation kinetics and defect structures, which will be discussed further in this paper. The gradual increase in chromium formation with voltage indicates how electric fields may promote selective oxidation, further affecting the alloy's resistance to corrosion.

https://doi.org/10.31436/iiumej.v26i2.3577

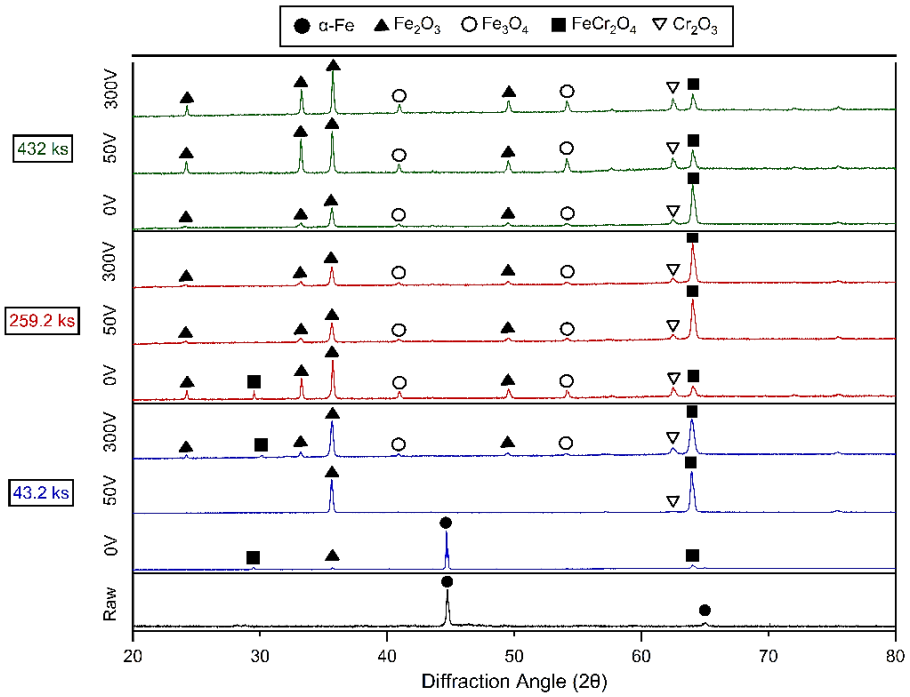

Figure 2. XRD patterns of all samples exposed at 650°C after 43.2, 259.2, and 432 ks of exposure with the proposed voltage supplied. The figure also includes the XRD pattern of the raw sample.

3.2. SEM Analysis

The morphology of the sample at the proposed timeframe was summarized in Figure 3. A red dashed line indicates the interphase boundary between the alloy, inner scale, and outer scale. For ease of discussion, the inner scale will be referred to as magnetite, while the outer scale is hematite, and the term will be used interchangeably in the discussion. Based on Figure 3, all samples show the presence of oxide layers at various supplied external voltages. It was also observed that the voids' shape was irregular, and some aligned in a lath-like pattern at a specific oxide thickness. A clear example of voids and lath-like patterns can be seen in Figure 4.

Voids in the inner and outer oxide scale are formed due to the ionic flux. A study by Ueda et. al. [11] stated that the partial pressure of oxygen can affect the void formation. The higher the oxygen partial pressure, the higher the oxygen chemical potential; hence, more voids are formed. Even though the oxygen partial pressure of this experiment is high (2.1×10^4 Pa), there is a presence of voids in the outer scale, and only a few appear in the inner scale. In addition, Taniguchi [12] proposed that the oxide expanded under a compressive force if the volume of oxide formed by the metal exceeded unity. If the ratio, however, were less than one, the resulting oxide would expand under tensile stress. As a result, a porous oxide coating develops. The oxide layer was either island-like or layer-by-layer when subjected to high temperatures [13].

https://doi.org/10.31436/iiumej.v26i2.3577

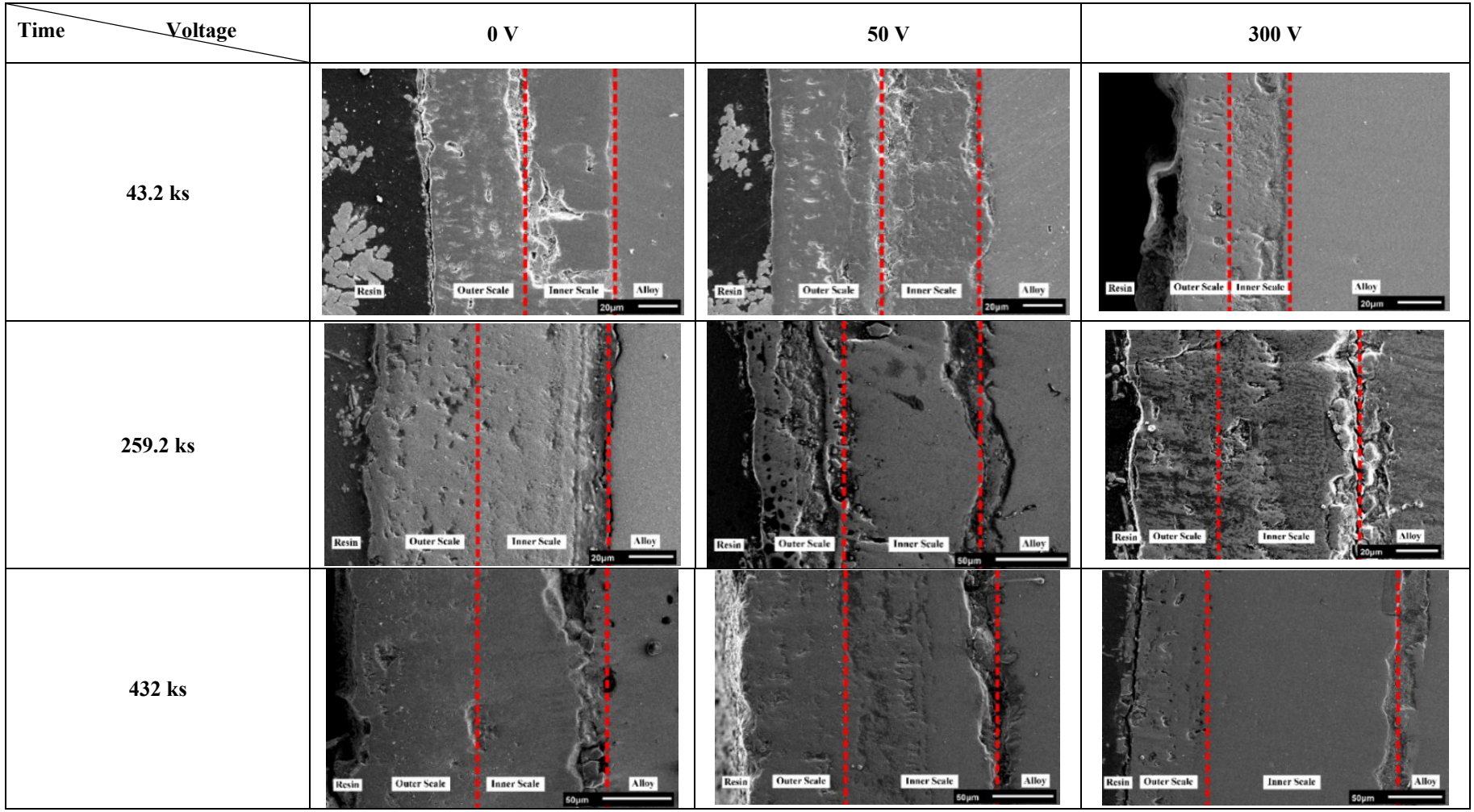

Figure 3. Cross sectional micrograph of T91 alloy through various timeframe and voltage.
Red dashed line indicates the interphase boundary.

https://doi.org/10.31436/iiumej.v26i2.3577

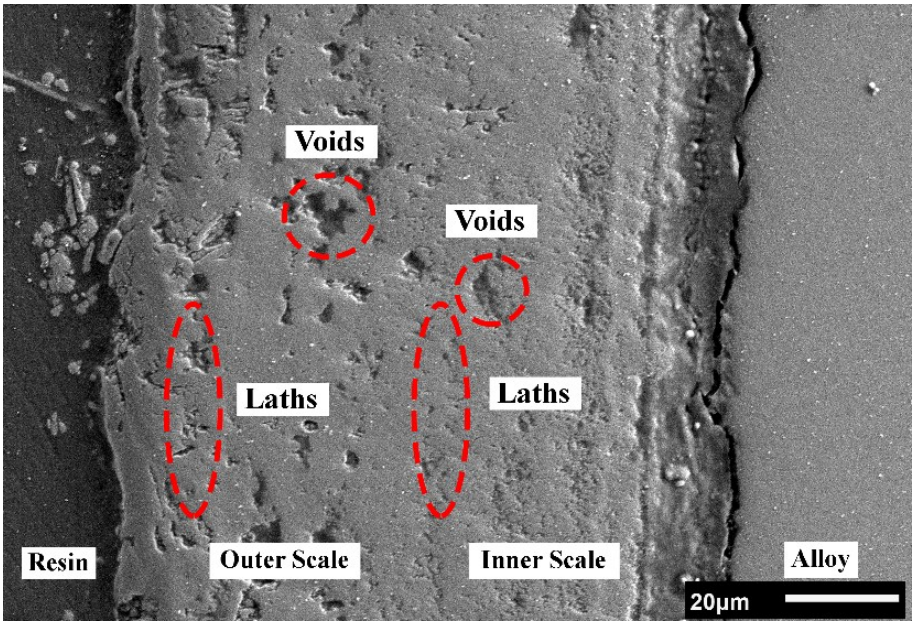

Figure 4. Formation of voids and laths from one of the cross sections exposed to the proposed condition. The image was taken from a sample exposed for 259.2 ks at 0V.

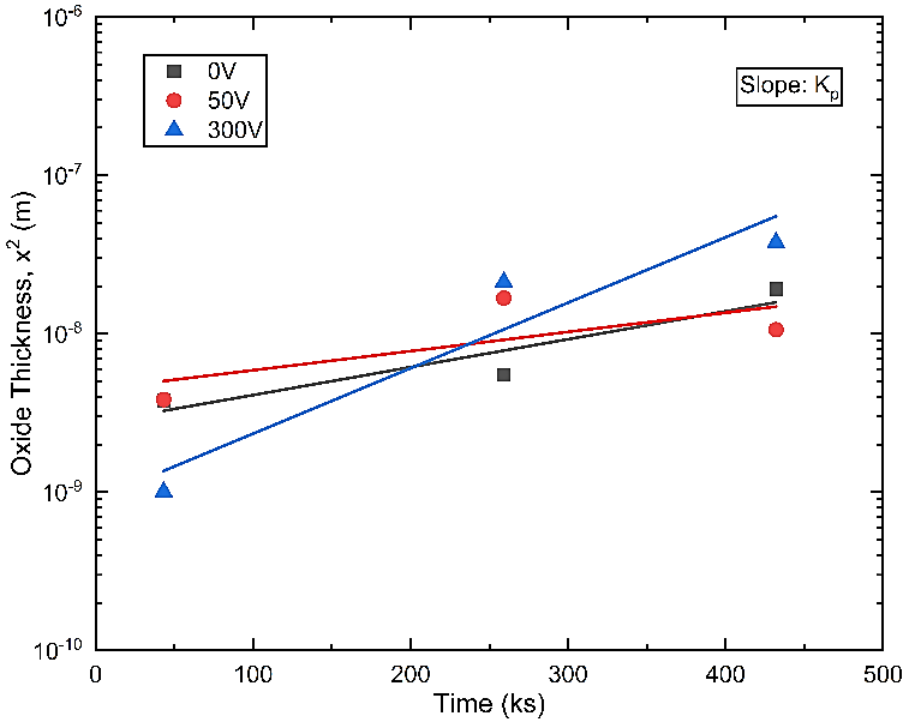

Figure 5. Overall oxide thickness vs Time.

Figure 5 shows the parabolic plots of the overall oxide thickness from the perspective of the weight gain of the sample. It shows a sharp increase at the beginning phase and then slowly gains weight up to 432 ks. The weight gain for the sample exposed to 0V does not follow the parabolic pattern, especially at 259.2 ks of exposure. This was due to oxide spallation, which causes it to become fragile during the final weight measurement. Overall, it indicates that almost all oxide scales formed obey the parabolic rate law. From the cross-section of the sample, the thickness of oxide scales can be determined to calculate the parabolic rate constant,

K_p. The K_p values for 0V, 50V and 300V were 3.83×10^{-14} m^2/s, 2.17×10^{-14} m^2/s and 9.25×10^{-14} m^2/s respectively.

3.3. Volume Fraction of Voids in Oxide Scale

Figure 6 shows the graphical representation of the volume fraction of voids for the sample's overall phase. The image illustrates that the volume percentage of voids and the governing equations are in good agreement. It also shows that as exposure time increases, void formation decreases. Overall, the formation of voids has decreased by 17%.

Similarly, as the voltage supplied increased, void formation on the oxide layers also decreased. Generally, oxygen ions from the air will diffuse into the sample when exposed to a high-temperature environment. Iron and chromium ions within the sample will also diffuse to the surface. The difference in flux between iron, chromium, and oxygen ions triggers a faster reconfiguration for some of them, causing slower-moving ions to have difficulty moving and redistributing themselves. Thus, it will lead to the accumulation of voids. However, if external driving forces are present, for this case, externally supplied voltage, the flux increased as well. Hence, the diffusion process will speed up, causing void formations to be reduced.

For T91 alloy, chromium reacts with oxygen and will form a passive layer called chromia, which prevents further oxidation [14]. Chromia has a much slower diffusion rate than other oxide layers. Thus, some of the iron ions managed to react with oxygen to form an oxide layer [15]. By inducing voltage onto the sample, the flux of chromia can be accelerated, allowing it to reach the surface quicker and participate in oxide layer formation, enhancing both the passive layer and resistance against void formation and corrosion. Figure 7 shows the overall void percentage of T91 alloy decreases linearly with time.

A plot of overall void percentage vs voltage is shown in Figure 8. The correlation indicates that void percentage decreases exponentially as voltage increases. Conversely, Figure 8 also illustrates that increasing the voltage causes the void percentage to plateau, eventually reaching a limit — indicating that beyond a certain point, applying higher voltage does not significantly affect the void percentage.

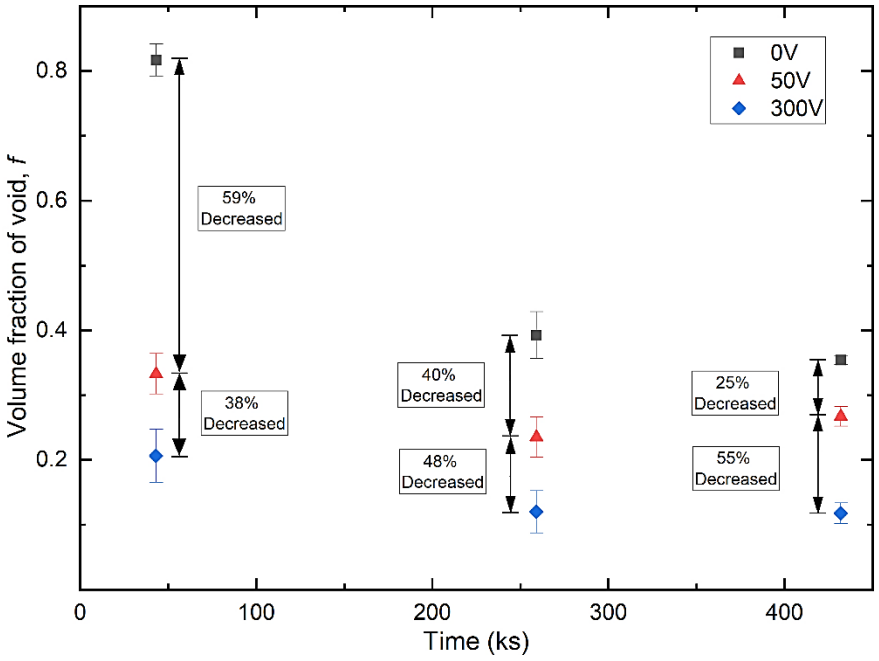

Figure 6. Volume fraction of void for overall phase of the sample.

https://doi.org/10.31436/iiumej.v26i2.3577

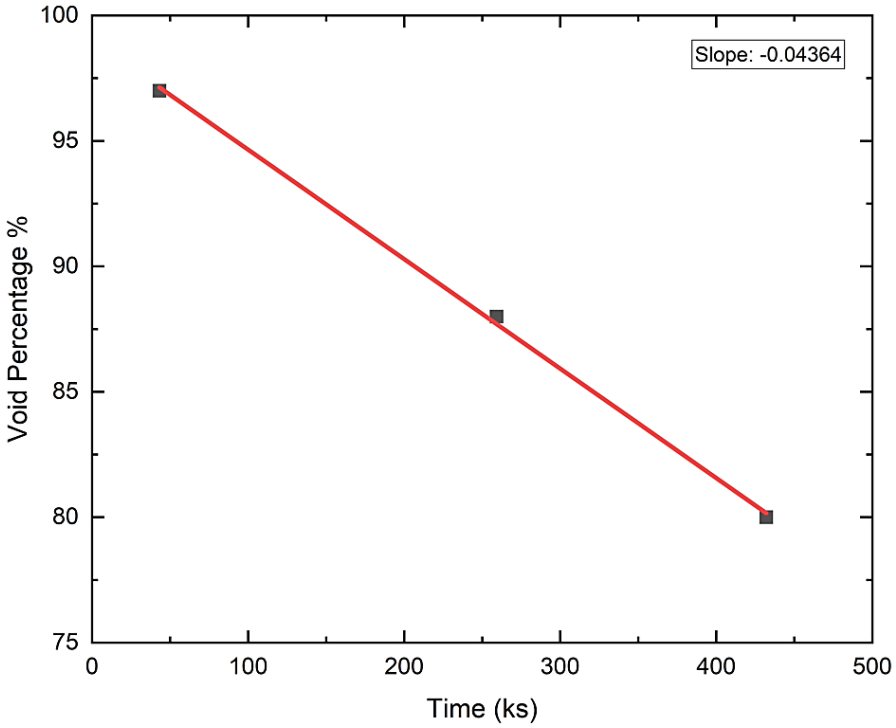

Figure 7. Overall void percentage vs Time.

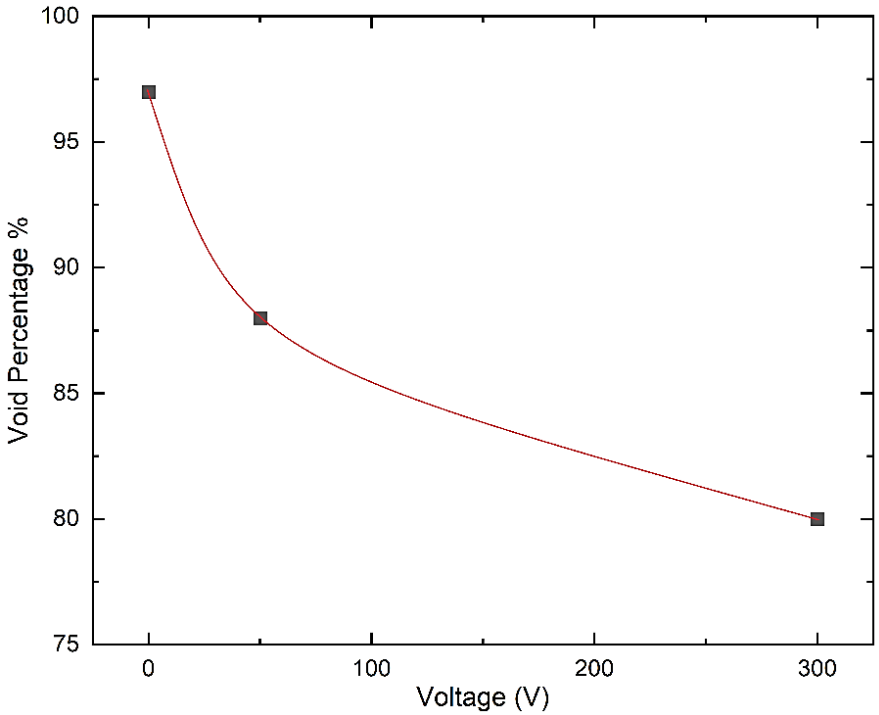

Figure 8. Overall void percentage vs Voltage.

Based on the graphs obtained in Figures 6, 7, and 8, a more detailed analysis of the void percentage in hematite and magnetite layers can be conducted, as illustrated in Figures 9 and 10. These figures clearly show a distinction: a higher volume of voids is formed in hematite compared to magnetite. This phenomenon can be explained by several factors related to these two oxide layers' crystal structure and properties.

https://doi.org/10.31436/iiumej.v26i2.3577

Magnetite has a spinel structure and consists of both Fe^{2+} and Fe^{3+} ions. This structure allows more oxygen vacancies and defects within the oxide lattice [16]. Hence, magnetite tends to exhibit a higher probability of void formation because it can facilitate the movement of iron ions. In contrast, hematite has an alpha-corundum crystal structure and contains only Fe^{3+} ions. Hematite is more compact and less prone to the formation of defects and voids [17]. This is not the case when an external voltage has been supplied. The volume fraction of voids for both layers appeared to decrease as a higher voltage was supplied. Plus, the exponential pattern on the volume fraction of void in magnetite phase appears steeper than that of hematite.

At exposed temperature, magnetite demonstrates an intriguing interplay between its magnetic and electrical properties, being a ferrimagnetic material that inherently exhibits both. Due to its mixed-valence compound, it creates a charged imbalance in the crystal lattice, resulting in the presence of electrical conductivity. As noted by Radoń et al. [18], rising temperatures significantly enhance the electrical conductivity of magnetite due to increased thermal energy, which facilitates a higher concentration of charge carriers. When combined with an applied external voltage, the resulting induced current accelerates diffusion within the magnetite layer, thereby reducing void formation.

On the contrary, hematite behaves as paramagnetic at temperatures above the Neel temperature (TN ≈ 955K), where the magnetic moments become disordered, resulting in no long-range magnetic ordering [19]. Therefore, hematite is considered an insulator or weakly conducting material as well as having a wide bandgap, which restricts the flow of electrical current [20]. Due to the mentioned hematite properties, an increase in voltage supplied shows a less significant steep slope, as shown in Figures 9 and 10. Moreover, when the voltage was set to 300V, their volume fraction of void shows an almost linear pattern (Figure 10). Overall, the effect of inducing different amounts of voltage onto T91 alloy shows that as the voltage supplied increases, it speeds up the diffusion rate of magnetite, causing less formation of voids, and vice versa for hematite.

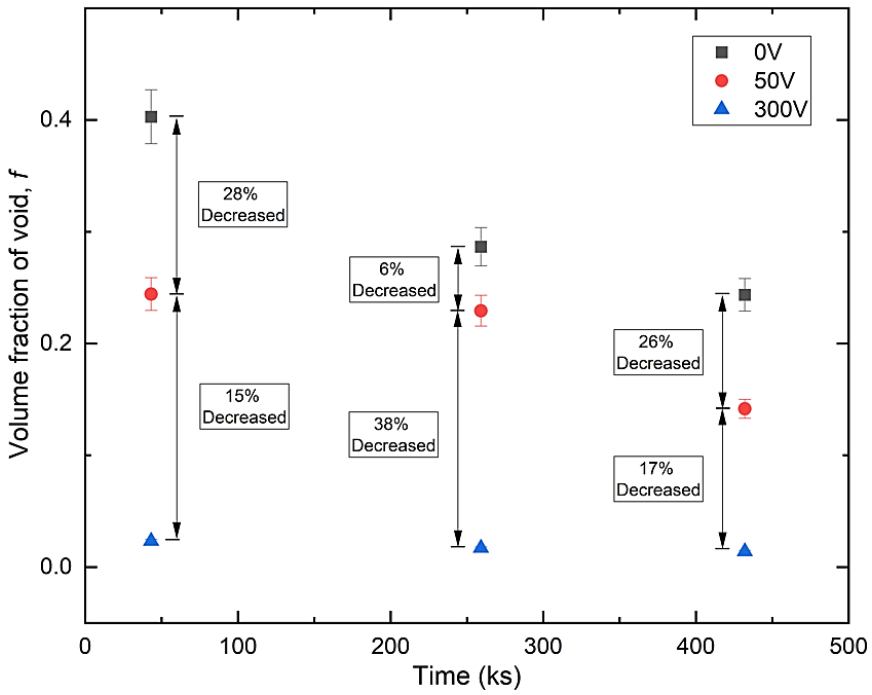

Figure 9. Void Percentage for all samples according to the hematite layer.

https://doi.org/10.31436/iiumej.v26i2.3577

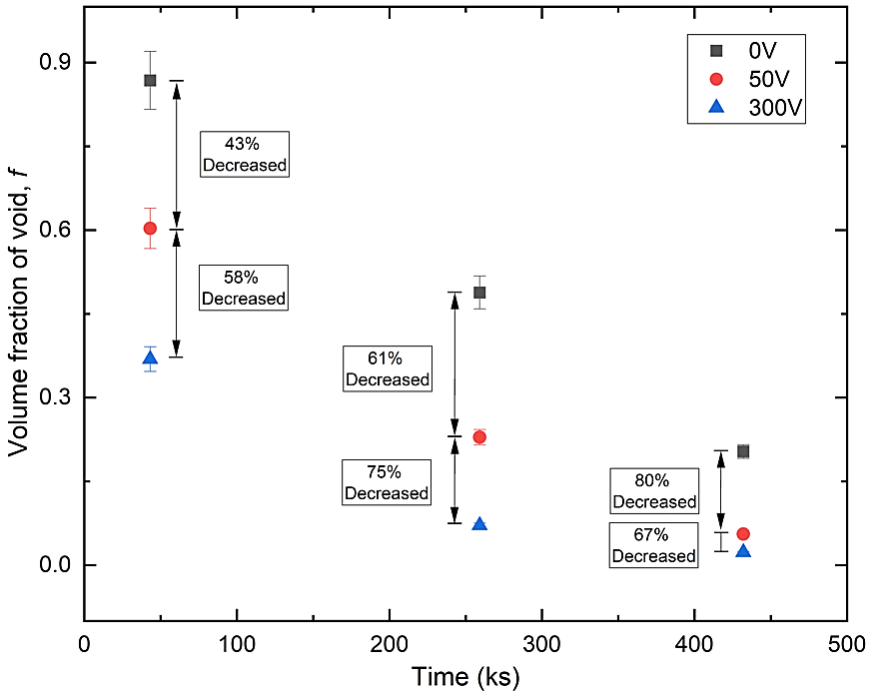

Figure 10. Void Percentage for all samples according to the magnetite layer.

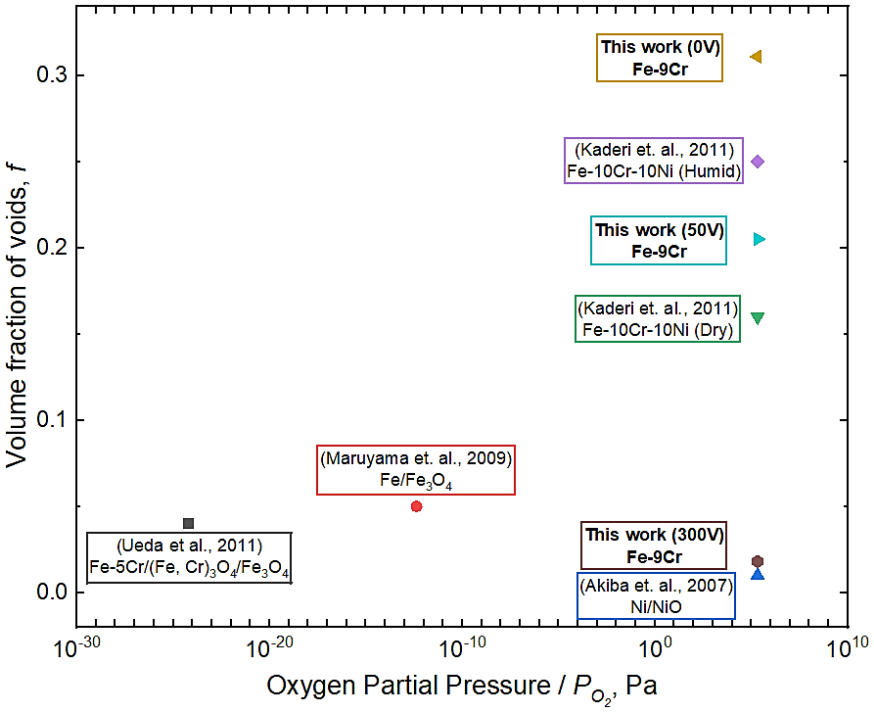

Figure 11. Comparison of volume fraction of voids on the outermost scale with other works.

Figure 11 shows a summary of work done on the volume fraction of voids on the outermost scale of the sample with respect to oxygen partial pressure, P_{O_2}. A study on void formation at the magnetite scale conducted by Maruyama et al. [3] and Ueda et al. [18] showed a very small range of voids formed in the range of 0.05 to 0.06. Note that these two studies were conducted in a controlled environment. In contrast, a study on void formation of NiO scale by Akiba et al. [21] and void on Fe-Cr-Ni alloy by Kaderi et al. [7] was done in normal air and is comparable

with this work. Note that the volume fraction of void on the outer scale is much smaller when voltage is supplied.

4. CONCLUSION

T91 alloy has been exposed to a high-temperature corrosion environment at 923 K. The samples were subjected to impressed voltages of 0V, 50V, and 300V at 43.2 ks, 259.2 ks, and 432 ks. XRD analysis confirmed the formation of oxide layers in all conditions, with phase identification indicating the presence of hematite, magnetite, and chromium. SEM cross-sectional analysis revealed the development of voids within oxide scales, with void formation quantified at both the overall scale and within individual phases.

Oxidation kinetics, assessed through oxide thickness measurements, followed the parabolic law, verifying that solid-state diffusion governed the reaction. Overall K_p value for samples exposed at 0V, 50V, 100V and 300V were 3.83×10^{-14} m^2/s, 2.17×10^{-14} m^2/s and 9.25×10^{-14} m^2/s respectively. This suggested that 50V suppressed oxidation rates while higher voltages (300V) accelerated diffusion kinetics, leading to increased oxidation rates. The enhancement of oxidation at 300V can be attributed to increased mobility of oxygen and metal cations under the influence of the external electric field, which facilitates faster oxide scale growth. SEM images also revealed that voids formed in all samples.

The void percentage for the overall, hematite, and magnetite layers has been calculated. The result shows that overall void formation decreased by 17% as exposure time increases, and a smaller number of voids was observed on magnetite phases compared to hematite. This is due to magnetite's higher electrical conductivity, which enhances diffusion and reduces void formation under applied voltage, and vice versa for hematite. At 300V, void formation in hematite stabilized while magnetite showed a steeper decline. These findings confirm that applied voltage influences oxidation behaviour by accelerating diffusion in magnetite, reducing void formation, while having a lesser effect on hematite.

ACKNOWLEDGEMENT

The author would like to acknowledge that no external funding sources were utilized in the conduct of his research. This work was carried out independently without financial support from organizations or institutions.

REFERENCES

[1] S. G. Subraveti, S. Roussanaly, R. Anantharaman, L. Riboldi, and A. Rajendran, "Techno-economic assessment of optimised vacuum swing adsorption for post-combustion CO_2 capture from steam-methane reformer flue gas," *Sep Purif Technol*, vol. 256, Feb. 2021, doi: 10.1016/j.seppur.2020.117832.

[2] Y. Li, J. Du, L. Li, K. Gao, X. Pang, and A. A. Volinsky, "Mechanical properties and phases evolution in T91 steel during long-term high-temperature exposure," *Eng. Failure Analysis*, vol. 111, Apr. 2020, doi: 10.1016/j.engfailanal.2020.104451.

[3] T. Maruyama, M. Ueda, and K. Kawamura, "Void formation in the growing scale induced by the divergence of the diffusive ionic flux in high temperature oxidation of metals," *Defect Diffus. Forum*, Trans Tech Publications Ltd, 2009, pp. 1–13. doi: 10.4028/www.scientific.net/DDF.289-292.1.

[4] T. Maruyama, K. Akiba, M. Ueda, and K. Kawamura, "Void formation in growing oxide scales with Schottky defects and p-type conduction," *Mater. Sci. Forum*, vol. 595–598, pp. 1039–1046, 2008, doi: 10.4028/www.scientific.net/MSF.595-598.1039.

[5] R. Schlögl and F. Helfferich, “Comment on the significance of diffusion potentials in ion exchange kinetics,” *J Chem. Phys.*, vol. 26, no. 1, pp. 5–7, 1957, doi: 10.1063/1.1743264.

[6] Y. Jin, Y. Zhang, and Y. Liu, “Corrosion reaction kinetics and high-temperature corrosion testing of contact element strips in ultra-high voltage bushing based on the phase-field method,” *IET Gener. Transm. Distrib.*, vol. 16, no. 2, pp. 249–260, 2022, doi: 10.1049/gtd2.12487.

[7] A. Kaderi, A. Zaki, M. Zainal, H. Ani, and R. Othman, “Observation on Void Formed in Oxide Scale of Fe-Cr-Ni Alloy at 1073K in Dry and Humid Environments,” *IIUM Eng. J.*, vol. 12, no. 5, pp. 69–78, 2011, doi: 10.31436/iiumej.v12i5.235.

[8] M. H. B. Ani, T. Kodama, M. Ueda, K. Kawamura, and T. Maruyama, "The effect of water vapor on high temperature oxidation of Fe-Cr alloys at 1073 K," *Mater. Trans.*, vol. 50, no. 11, pp. 2656–2663, 2009, doi: 10.2320/matertrans.M2009212.

[9] S. Nasrazadani and A. Raman, "The application of infrared spectroscopy to the study of rust systems—II. Study of cation deficiency in magnetite (Fe_3O_4) produced during its transformation to maghemite (γ-Fe_2O_3) and hematite (α-Fe_2O_3)," *Corrosion Sci.*, vol. 34, no. 8, pp. 1355–1365, 1993, doi: 10.1016/0010-938X(93)90092-U.

[10] T. Simmonds and P. C. Hayes, “Isothermal Oxidation of Magnetite to Hematite in Air and Cyclic Reduction/Oxidation Under Carbon Looping Combustion Conditions,” *Metall. Mater. Trans. E*, vol. 4, no. 2–4, pp. 114–122, Dec. 2017, doi: 10.1007/s40553-017-0111-7.

[11] M. Ueda, K. Kawamura, and T. Maruyama, "Void formation in magnetite scale formed on iron at 823 K—Elucidation by chemical potential distribution," *Mater. Sci. Forum*, vol. 523, pp. 37–44, 2006, doi: 10.4028/www.scientific.net/MSF.522-523.37.

[12] S. Taniguchi, “Stresses developed during the oxidation of metals and alloys,” *Trans. Iron Steel Inst. Jpn.*, vol. 25, pp. 3–13, 1985, doi: 10.2355/isijinternational1966.25.3.

[13] A. Fluri, D. Pergolesi, V. Roddatis, A. Wokaun, and T. Lippert, "In situ stress observation in oxide films and how tensile stress influences oxygen ion conduction," *Nat. Commun.*, vol. 7, no. 1, p. 10692, 2016, doi: 10.1038/ncomms10692.

[14] R. D. Armstrong, “Electrochemical Dissolution,” *Encyclopedia of Materials: Science and Technology*. Elsevier, pp. 2521–2525, 2001. doi: 10.1016/B0-08-043152-6/00456-3.

[15] T. Jonsson (2007) Microscopy of High Temperature Oxidation of Iron and Some Stainless Steels PhD thesis. Chalmers University of Technology. Retrieved from https://research.chalmers.se/en/publication/40412.

[16] R. Arras, B. Warot-Fonrose, and L. Calmels, “Electronic structure near cationic defects in magnetite,” *J. Phys. Condens. Matter*, vol. 25, no. 25, Jun. 2013, doi: 10.1088/0953-8984/25/25/256002.

[17] K. R. Tolod, S. Hernández, E. A. Quadrelli, and N. Russo, “Visible light-driven catalysts for water oxidation: Towards solar fuel biorefineries,” in *Studies in Surface Science and Catalysis*, vol. 178, S. Albonetti, S. Perathoner, and E. A. Quadrelli, Eds., Elsevier, 2019, pp. 65–84, doi: 10.1016/B978-0-444-64127-4.00004-5.

[18] A. Radoń et al., “Influence of magnetite nanoparticles shape and spontaneous surface oxidation on the electron transport mechanism,” *Materials*, vol. 14, no. 18, Sep. 2021, doi: 10.3390/ma14185241.

[19] D. Varshney and A. Yogi, “Structural and Electrical conductivity of Mn doped Hematite (α-Fe_2O_3) phase,” *J. Mol. Struct*, vol. 995, no. 1–3, pp. 157–162, May 2011, doi: 10.1016/j.molstruc.2011.04.011.

[20] J. Engel and H. L. Tuller, “The electrical conductivity of thin film donor doped hematite: From insulator to semiconductor by defect modulation,” *Phys. Chem. Chem. Phys.*, vol. 16, no. 23, pp. 11374–11380, Jun. 2014, doi: 10.1039/c4cp01144a.

[21] K. Akiba, M. Ueda, K. Kawamura, and T. Maruyama, “Quantitative prediction of voids formation in a growing nickel oxide scale at 1371 K,” *Mater. Trans.*, vol. 48, pp. 2753–2761, Oct. 2007, doi: 10.2320/matertrans.MER2007122.